Revista Ingeniería de Construcción RIC
Vol 38 Nº2 2023
www.ricuc.cl
DOI: 10.7764/RIC.00073.21

ENGLISH VERSION

Assessment and monitoring of moisture content variation in compacted tropical soil using GPR data

Evaluación y monitoreo de la variación del contenido de humedad en suelo tropical compactado usando datos GPR

J. Pizarro Marchenaa*[1,] https://orcid.org/0000-0003-1455-0241
M. T. Françosob **, https://orcid.org/0000-0002-7849-355X
H. Moraes Treiberc**, https://orcid.org/0000-0002-4859-5213
N. de Oliveira Stenicod**, https://orcid.org/0000-0001-9369-626X

* Faculty School of Construction Engineering, Costa Rica Institute of Technology, Cartago, COSTA RICA
** Engineering, Architecture and Urban Design, University of Campinas, Campinas, BRAZIL

Fecha de Recepción: 19/07/2022
Fecha de Aceptación: 17/02/2023
Fecha de Publicación: 02/08/2023
PAG: 334-349

Abstract

The rapid deterioration and unsatisfactory performance of highway pavements are also related to the variation and excessive accumulation of moisture in the subgrade and in constituent layers. Hence, moisture control is essential to ensure, in part, the durability and good performance of these types of structures. Ground Penetration Radar (GPR) has proven to be a useful potential alternative for this purpose, given its non-invasive characteristics, preserving the integrity of the site under observation, in addition to the ability to quickly and continuously collecting data. This study aims at evaluating the sensitivity of the GPR to moisture changes and to investigate the influence that calibration models have on predicting moisture content in a compacted tropical soil. Deformed lateritic soil samples were used and subjected to physical properties' characterization and compaction tests. A 1600 MHz antenna GPR was used for data acquisition in a controlled laboratory environment. On the whole, the results showed that GPR is a promising alternative, with both satisfactory accuracy in moisture assessment and sensitivity when monitoring changes in moisture content in compacted soils.

Keywords: *GPR; moisture content; dielectric permittivity; tropical soil, calibration models.*

Resumen

El rápido deterioro y el desempeño insatisfactorio de los pavimentos, también, están relacionados con la variación y acumulación excesiva de la humedad en la subrasante y en sus capas constituyentes. De ahí que el control de la humedad sea fundamental para asegurar, en parte, la durabilidad y el buen comportamiento de este tipo de estructuras. El Georradar (GPR) ha demostrado ser una potencial alternativa útil para este propósito, dadas sus características no invasivas, preservando la integridad del sitio bajo observación, además de la capacidad de recolectar datos de manera rápida y continua. Este estudio tiene como objetivo evaluar la sensibilidad del GPR a los cambios de humedad e investigar la influencia que tienen los modelos de calibración en la estimación del contenido de humedad en un suelo tropical compactado. Se utilizaron muestras de suelo laterítico deformado y se sometieron a ensayos para la caracterización de sus propiedades físicas y compactación. Se utilizó una antena GPR de 1600 MHz para la adquisición de datos en un ambiente de laboratorio controlado. En general, los resultados mostraron que el GPR es una alternativa promisoria, con precisión satisfactoria en la evaluación de la humedad y sensibilidad al monitorear cambios en el contenido de humedad en suelos compactados.

Palabras clave: *GPR; contenido de humedad; permitividad dieléctrica; suelo tropical; modelos de calibración.*

[1] *Corresponding author:*
School of Construction Engineering, Costa Rica Institute of Technology, Cartago, COSTA RICA
ipizarro@itcr.ac.cr

1. Introduction

Even a properly designed pavement, built to meet structural and functional demands, will eventually present problems early on because of climatic factors. Intense rainfall and temperature variation (so characteristic of tropical countries) are the major causes of the presence of water inside the road pavement, generating thus a direct effect on the behavior of materials and soils which are highly sensitive to changes in moisture content.

Research shows that the rapid deterioration and unsatisfactory road pavement performance are also related to the variation and accumulation of excessive moisture in the subgrade and constituent layers (Benedetto and Benedetto, 2002); (Pereira, 2003); (Al-Qadi et al., 2004); (Azevedo, 2007); (Larrahondo et al., 2008);(Bastos, 2013). Some of the most commonly known effects are a reduction in the stiffness of granular base and subbase course, volume changes, loss of bearing capacity of the subgrade and variation in the resilience module (Al-Qadi et al., 2004);(Evans, Frost and Morrow, 2012). These effects are apparent in the pavement surface course as rutting, cracking, potholes, the presence of pumped-thin material (pumping), steps and concrete slab rupture (Suzuki et al., 2013).

Although the effect of the presence of water on pavement is a widely studied topic, there is little research dedicated to the investigation of new techniques that allow tracking the behavior and action of water within the pavement through "in situ" monitoring. The techniques traditionally applied in monitoring moisture content in roads (core sampling, neutron and capacitance probes, or resistance devices), are accurate, but are costly, time-consuming and invasive, with little representative information when analyzing long stretches in the long run (Berthelot et al., 2010; Benedetto et al., 2017). Researchers agree that non-destructive methods (NDM) are potentially the most efficient, effective, and reliable techniques, besides providing continuous information and preserving the integrity of the site under observation (Loulizi, 2001); (Grote et al., 2005); (Berthelot et al., 2010); (Benedetto and De Blasiis, 2010); (Plati and Loizos, 2013).

GPR is one of the most widespread geophysical methods employed in shallow prospection and adopted in engineering for the study and evaluation of the state of civil infrastructure. It is a non-destructive technique, with the means to collect data quickly and continuously, besides presenting high flexibility of use and reliability in the results (Grote et al., 2002); (D'Amico et al., 2010); (Benedetto et al., 2017). After the year 2000, technological advances and improvements in computational capabilities led to the emergence of GPR applications in civil infrastructure (Wai-Lok Lai et al., 2017). The traditional and most widespread application in transportation infrastructure is related to pavement layer thickness determination and more recently in the state's assessment and condition of its structure and foundation.

The primary aim of this study is to evaluate GPR sensitivity to moisture changes in a compacted tropical soil and to analyze, in terms of accuracy, the influence that calibration models relating dielectric permittivity to moisture have on moisture content prediction in a controlled laboratory environment. For this purpose, lateritic soil samples were compacted at standard Proctor energy and optimum moisture content. The soil moisture loss at room temperature was monitored with GPR data and by the oven drying method. The resulting wave traces from GPR data were used to estimate the propagation velocity and determine at the first stage the dielectric permittivity and later the moisture content using calibration models.

2. Theoretical Framework

GPR uses the principle of electromagnetic (EM) wave transmission with center frequencies ranging from 10 MHz to 2.5 GHz. The EM wave is generated and radiated from a transmitting antenna, traveling through the medium at a velocity that is defined primarily by the properties of the medium. The wave propagates until it reaches a medium with different electrical properties, generating its dispersion. Part of the energy is reflected and detected by a receiving antenna, while the rest of the energy continues its journey (Figure 1). According to (Daniels, 2000), the relationship between the velocity of wave propagation and the electromagnetic properties of materials (magnetic permeability, electrical conductivity, and dielectric permittivity) is the fundamental basis for the use of GPR.

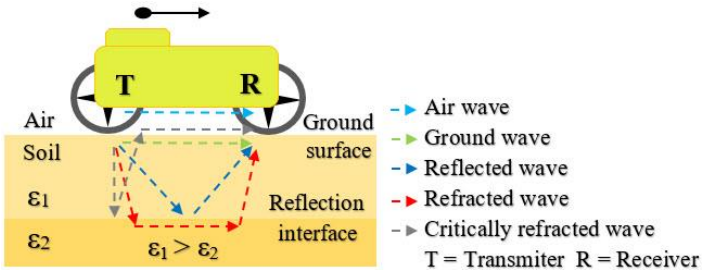

Figure 1. *GPR signal propagation in a two-layer soil with different dielectric permittivity*

Generally, mineral soil magnetic properties are the same as in free space and magnetic permeability (μ_r) is commonly considered equal to the unit ($\mu_r = 1$), in the frequency range from MHz to GHz (Mohamed, 2008; Curioni, 2013). The electrical conductivity (σ) of the medium contributes to the attenuation of the GPR pulse and its reflection. However, the most important electrical property influencing GPR data is the dielectric permittivity (ε_r) and its effect on the velocity of wave propagation in the medium (Saarenketo, 2006).

The behavior of materials such as soil, comprising three phases (solid, air and liquid), in the presence of an electromagnetic wave is complex, since it can present both dielectric and conductive properties. The electrical properties are controlled by the microscopic scale behavior of its components, which combine to produce an overall response of the material (Muller, 2016).

The electrical conductivity (σ) of soils varies between 0,001 - 2 dSm^{-1} for low frequencies (Hz to kHz) and the relative dielectric permittivity (ε_r) presents values between 3 - 50 for high frequencies (MHz to GHz). Thus, electrical conductivity at low frequencies (Hz - kHz), and dielectric permittivity at high frequencies (MHz - GHz), are the electrical properties commonly measured and modeled to assess moisture content in soils (Friedman, 2011).

Accurate estimations of moisture content, using electromagnetic techniques, require accurate calibration models that allow relating the dielectric permittivity (ε_r) with the volumetric moisture content (θ_v). These models can be empirical, theoretical or theoretical-empirical (Ekblad and Isacsson, 2007). Models resulting from empirical procedures obtained from laboratory and field data are less complex than theoretical models and can apply to a variety of soil textures under different moisture conditions. The most widely used empirical equation, and probably the most widely cited, was developed by (Topp et al., 1980), (Equation (1).

$$\theta_v = -5{,}3x10^{-2} + 2{,}92x10^{-2}\varepsilon_r - 5{,}5x10^{-4}\varepsilon_r^2 + 4{,}3x10^{-6}\varepsilon_r^3 \quad (1)$$

where, θ_v= volumetric moisture content [cm^3 cm^{-3}] and ε_r= relative dielectric permittivity.

Other models have been developed based on the approach of (Topp et al., 1980). This is the case of (Nadler et al.,1991), (Roth et al., 1992), (Jacobsen and Schjønning, 1993). In the pavement-specific field, the model of (Jiang and Tayabj, 1999) (Equation (2), resulted from the laboratory study of soil samples collected from the subgrade of 28 experimental sections, in the Seasonal Monitoring Program (SMP) of long-term pavement performance (LTPP) of the U.S. Federal Highway Administration. More recently, (Pizarro et al., 2020) (Equation (3), developed a calibration model using tropical soils, with samples collected from the subgrade of different highways in the State of São Paulo, Brazil.

$$\theta_v = -0{,}8120 + 2{,}38682\varepsilon_r - 0{,}04427\varepsilon_r^2 + 2{,}92x10^{-4}\varepsilon_r^3 \quad (2)$$

$$\theta_v = -1{,}10x10^{-1} + 3{,}71x10^{-2}\varepsilon_r - 1{,}02x10^{-3}\varepsilon_r^2 + 1{,}28x10^{-5}\varepsilon_r^3 \quad (3)$$

where, θ_v= volumetric moisture content [cm^3 cm^{-3}] and ε_r= relative dielectric permittivity.

3. Materials and Methods

3.1. Materials

Deformed soil samples were collected directly from the subgrade during its regularization process, on the Prof. Zeferino Vaz Highway (SP-332) in the countryside of the State of São Paulo (22º22'21" S; 47º09'52" W / WGS-84).

The soils were submitted to tests of physical characterization, classification and compaction in the Soil Mechanics Laboratory of the Department of Infrastructure and Environment (InfrA) of the Faculty of Civil Engineering, Architecture and Urban Design (FEC) of UNICAMP. For the performance of the tests the procedures of the standards stated below, in (Table 1), were adopted.

***Table 1**. Tests and standards us ed in soil characterization and compaction*

Test	Standard number [citation]
Particle size analysis	NBR 7181 (ABNT, 2016d)
Determination of specific density	NBR 6458 (ABNT, 2016a)
Determination of Atterberg Limits	NBR 6459 (ABNT, 2016b) and NBR 7180 (ABNT, 2016c)
Soil compaction tests	NBR 7182 (ABNT, 2016e)

(Table 2) presents the physical characterization data and (Table 3) the soil classification in agreement with the Highway Research Board (HRB), Unified Soil Classification System (USCS) and the Tropical Soil Classification (MCT) (DNER, 1994a; DNER, 1994b; DNER, 1996).

***Table 2**. Summary of the physical characterization*

Sample name	ρ_s (g/cm³)	Granulometry (%)			Atterberg Limits (%)		
		Sand	Silt	Clay	LL	PL	PI
SP-332	2,75	62	13	25	25	14	10

ρ_s = Solids specific density, LL = Liquid limit, PL = Plastic limit, PI = Plasticity index.

***Table 3.** Soil Classification.*

Sample name	Classification		
	HRB	USCS	MCT
SP-332	A-6	SC	LG'

HRB = Highway Research Board, USCS = Unified Soil Classification System, MCT = Miniature, Compacted Tropical. SC = Clayey sand and LG' = lateritic clayey

Compaction tests were performed with the reuse of material at standard Proctor energy to determine the optimum moisture content and maximum dry density. A summary of the physical properties obtained is shown below in (Table 4).

***Table 4.** Physical properties of compacted soil.*

Sample	$\rho_{d\ Max.}$ (g/cm³)	$w_{optimum}$ (%)	$\theta_{v\text{-}optimum}$ (cm³cm⁻³)	e	n (%)	S_r (%)
SP-332	1,91	12,54	0,2395	0,44	30,5	78,5

$\rho_{d\ Max.}$ = Maximum dry density, $w_{optimum}$ = Optimum moisture content, $\theta_{v\text{-}optimum}$ = Optimum volumetric moisture content, e = void ratio, n = Porosity, Sr = Degree of Saturation.

A SIR-3000 control unit and a ground-coupled antenna with a 1600 MHz center frequency, all from GSSI, were used for data collection. The soil was molded and compacted in a 40 x 40 x 15 cm wooden box with 1,5 cm thick walls (Figure 2). The dimensions of the box were defined considering the minimum acquisition of 22 traces (2 traces/cm) in each survey and the dimensions of the antenna (cart + antenna), besides the physical properties ($\rho_{d-Max.}$ and $w_{optimum}$) of the sample to be compacted.

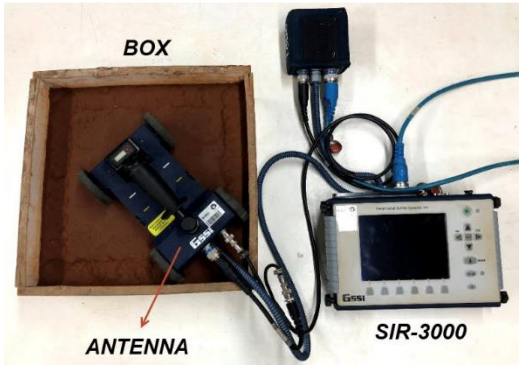

***Figure 2**. GPR system (SIR-3000 and 1600 MHz antenna) and wooden box with compacted soil.*

3.2. Methods

The propagation velocity of an electromagnetic wave (v_p) is determined by the dielectric permittivity (ε_r) and the relative magnetic permeability (μ_r), as follows (Huisman et al., 2003) (Equation 4):

$$v_p = \frac{c}{\sqrt{\varepsilon_r \, \mu_r \, \frac{1 + \sqrt{1 + \tan^2 \delta}}{2}}} \quad (4)$$

where, c is the velocity of an EM wave in free space [m/s] and the tangent loss ($\tan \delta$) is defined as the ratio between the imaginary part ($\varepsilon_r^{"}$), and the real part (ε_r') of the dielectric permittivity, which describes the degree of energy loss associated with the material (Equation (5).

$$\tan \delta = \frac{\varepsilon_r^{"} + \frac{\sigma_0}{2 \pi f \varepsilon_0}}{\varepsilon_r'} \quad (5)$$

where, f is frequency [Hz], ε_r' is the real part and $\varepsilon_r^{"}$ is the imaginary part of complex relative dielectric permittivity; σ_0 is the electrical conductivity at zero frequency and ε_0 is the permittivity in free space.

With non-magnetic, low-loss mineral soils (assuming relative magnetic permeability equal to unity, $\mu_r = 1$) (Van Dam et al., 2002), the propagation velocity (v_p) of the EM wave is given by (Equation 6):

$$v_p = \frac{c}{\sqrt{\varepsilon_r}} \quad (6)$$

where, c is the velocity of an EM wave in free space and ε_r is the dielectric permittivity of the medium. Any influence on the propagation velocity by magnetic permeability was disregarded, given the low content of minerals with magnetic properties present in the soil, according to the chemical analysis performed to determine the oxides of the elements, applying the X-ray fluorescence spectrometry technique.

(Figure 3) details the procedures adopted for soil preparation and compaction, as well as the data acquisition step using the GPR system.

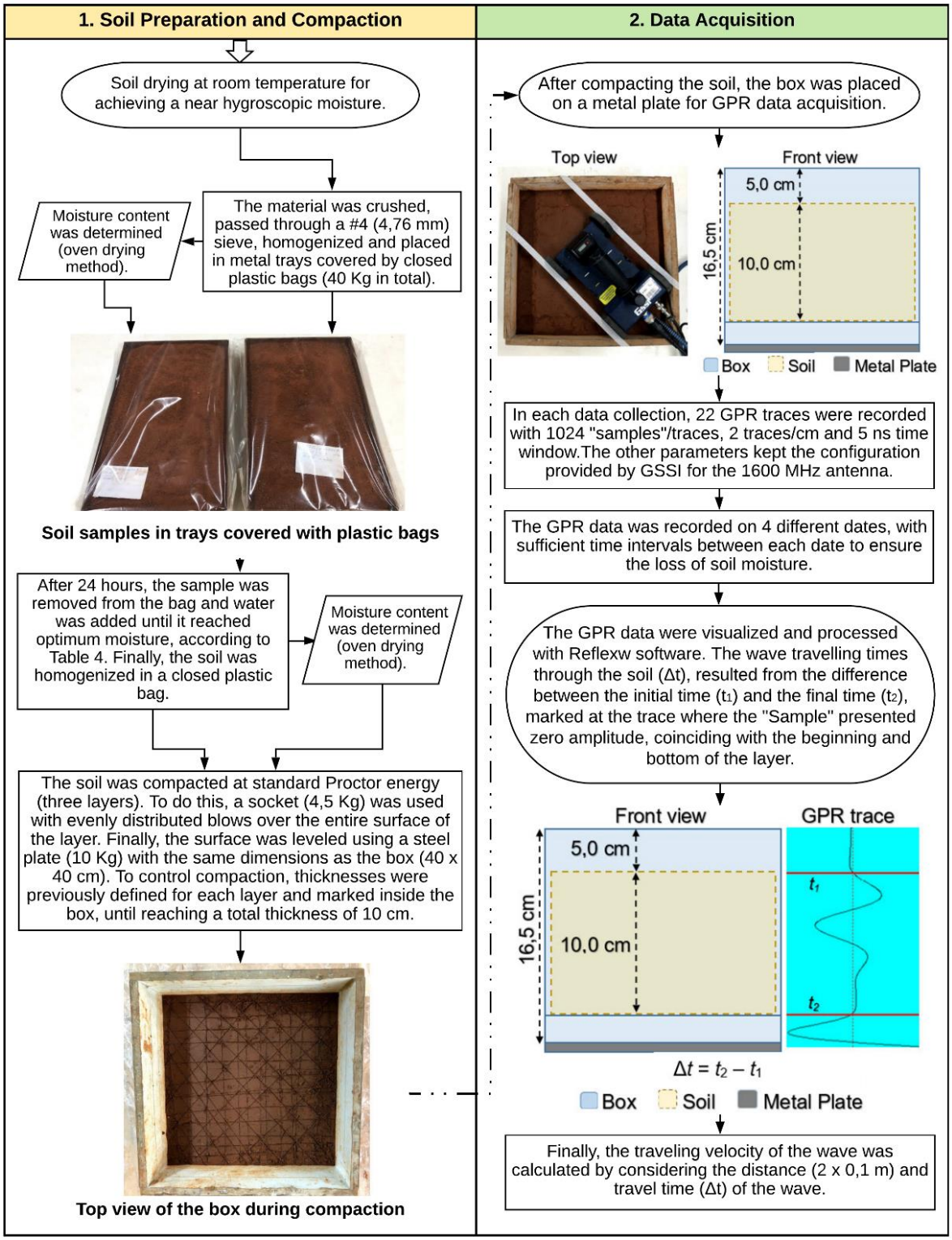

***Figure 3**. Schematic illustration of the procedures followed in soil preparation and data acquisition with the GPR system.*

With the propagation velocity known, the apparent relative dielectric permittivity of the soil (ε_{r-a}) was calculated using Eq. ((6). Then, the moisture content ($\theta_{v\,Estimated}$) was estimated by substituting the dielectric permittivity (ε_{r-a}) into the calibration models (Eqs. (1(2 and (3). Finally, $\theta_{v\,Estimated}$ was compared with the measured moisture ($\theta_{v\,Measured}$) using the oven drying method. The relationship between gravimetric and volumetric moisture is shown below in (Equation (7).

$$\theta_v = w \cdot \frac{\rho_d}{\rho_w} \qquad (7)$$

where, ρ_d is the dry soil specific mass [g/cm^3]; ρ_w is the water specific mass [g/cm^3] and w is the gravimetric moisture.

The gravimetric moisture content ($w_{Measured}$) was determined on three occasions, immediately after the GPR survey. For this purpose, it was necessary to extract samples from the compacted soil, with a sampler (Figure 4).

***Figure 4**. Extraction of a compacted soil sample to determine its moisture content by the oven drying method.*

4. Results and Discussion

The results obtained are presented and analyzed in this section. Four surveys were conducted over a 29-day period and soil samples were collected on three occasions to determine moisture content by the oven drying method. In each survey, 22 GPR traces were recorded. Using the Reflexw program, the gain was removed from the GPR data and the average trace from each survey was determined for wave travel time analysis. The travel time (Δt) resulted from the difference between the initial time (t_1) and the final time (t_2), defined by the beginning of the soil layer and the bottom of the layer at 10 cm depth, respectively. The times t_1 and t_2, were marked on the trace where the "Sample" presented amplitude close to zero (Figure 5).

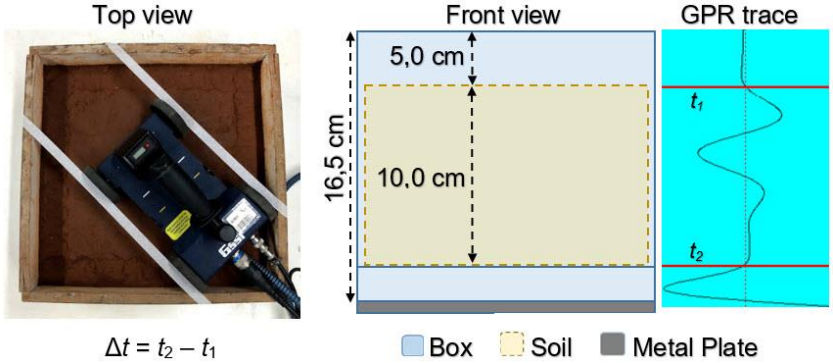

***Figure 5**. Top and front view of the box containing the compacted soil and the GPR trace signaling the initial and final time.*

The four traces with their respective collection order and times can be seen in (Figure 6). Two characteristics of the traces stand out, namely: a) the same trace shape in the four different moisture conditions (four peaks in the same shape and sequence), and b) the decrease in the apparent length of the trace that is directly related to the travel time and velocity of the wave.

The apparent length is another characteristic of the trace, as well as the shape and the amplitude. The variation in the apparent length was observed by comparing and analyzing the distinct traces at the same (arbitrary) propagation velocity. In other terms, the length scale (to the right of the trace in (Figure 6) was normalized by employing the same velocity (e.g., $v_{p-arbitrary}$ =1) when analyzing the four traces. As with the travel time (Δt), the apparent length (ΔAL), which corresponds to the stretch between the surface and the bottom of the soil layer, resulted from the difference between AL_1 and AL_2 (Figure 6).

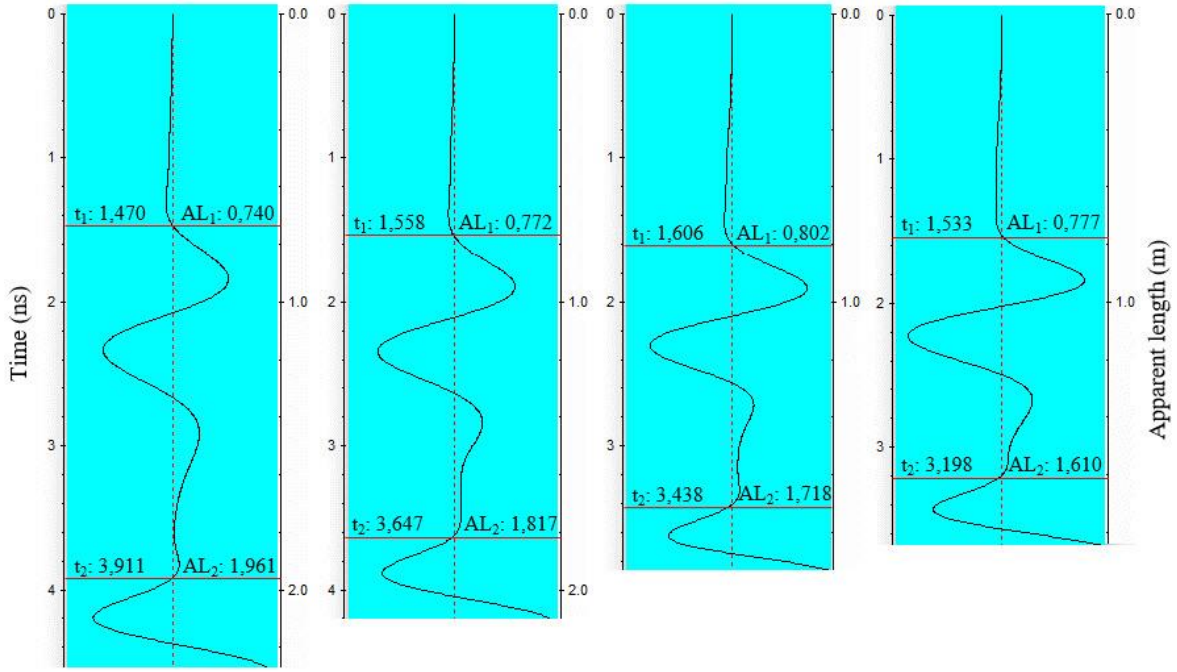

***Figure 6**. GPR traces with the initial and final times (t_1 and t_2), besides their respective apparent lengths, AL_1 and AL_2.*

The propagation velocity (v_p) was calculated using (Equation (8) and checked with that calculated using travel time (Δt). In all cases, the values of v_p were identical. Note from Equation 8that v_p does not depend on Δt, but it is necessary to know the layer thickness (LT). Just as it is also necessary to know LT to determine v_p using the travel time (Δt).

$$v_p = v_{p-arbitrary} \cdot \frac{LT}{\Delta AL} \qquad (8)$$

where, v_p= propagation velocity [m/ns]; $v_{p-arbitrary}$= arbitrary propagation velocity [m/ns]; LT = layer thickness [m]; ΔAL = apparent length of the trace that corresponds to the stretch between the surface and the bottom of the soil layer [m].
(

Table **5***) shows the propagation time (Δt), apparent length (ΔAL), propagation velocity (v_p) and apparent relative dielectric permittivity (ε_{r-a}) calculated from the trace analysis and expression (6.*

***Table 5**. Summary of the results obtained from the trace analysis.*

Trace number	Δt ***(ns)***	ΔAL ***(m)***	v_p ***(m/ns)***	ε_{r-a}
1	*2,441*	*1,221*	*0,0819*	*13,41*
2	*2,089*	*1,045*	*0,0957*	*9,83*
3	*1,832*	*0,916*	*0,1092*	*7,54*
4	*1,665*	*0,833*	*0,1201*	*6,24*

DOI: 10.7764/RIC.00073.21

The increase of the propagation velocity with the decrease of the apparent length was expected. Thus, the decrease in dielectric permittivity was also expected, coinciding with what was predicted by Eq. ((6) ($\varepsilon_{r-a} = \left(c/\boldsymbol{v_p}\right)^2$).

Figure 7 shows the relationship between propagation velocity (v_p) and apparent relative dielectric permittivity (ε_{r-a}) with propagation time (Δt) (Figure 7a) and with apparent length (ΔAL) (Figure 7b). It should be noted that the behavior and trend of the observations in both graphs are the same, regardless of whether propagation time or apparent length was used to determine at a first stage the propagation velocity (v_p) and then the apparent relative dielectric permittivity (ε_{r-a}).

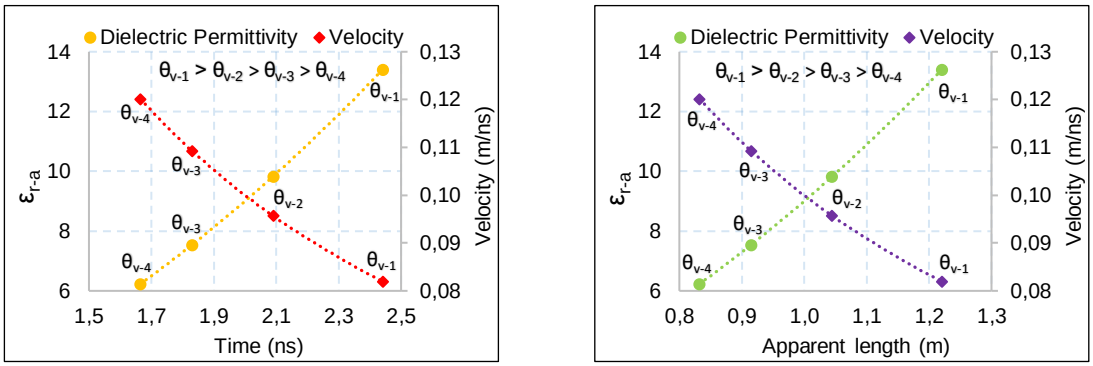

(a) *(b)*

***Figure 7**. Behavior and trend of the dielectric permittivity (ε_{r-a}) and propagation velocity (v_p) due to Δt and ΔAL.*

*In addition to the above, the behavior of the data presented in (Figure 6) and (Figure Figure **7**), shows the correlation between the propagation velocity and dielectric permittivity with the moisture content present in the soil. Thus, for a medium with a stable porous structure (defined as a low expansive and contractile soil, with low plasticity index, high sand content and high strength when compacted), the propagation velocity increases, and the permittivity decreases with moisture loss. In other terms, the velocity of the wave is conditioned by its interaction with the moisture content present in the propagation medium. The contribution of the liquid phase (water) to the soil dielectric permittivity varies, mainly, with the variation in the amount of water and according to the restriction on the freedom of rotation of the water molecules to polarize when close to the soil particles.*

*Once dielectric permittivity was determined, the volumetric moisture content ($\theta_{v\ Estimated}$) was estimated using (Equation (1), (Equation (2) and (Equation (3), and compared with the measured moisture content ($\theta_{v\ Measured}$) with the oven drying method (standard method). The results are shown in (Table 6). The differences and percentage errors that resulted from the comparison are shown in the graphs in (Figure 8) and (Figure Figure **9**)*

.

***Table 6.** Moisture contents estimated with the calibration models and those measured by the oven drying method.*

Trace	Model (cm^3cm^{-3})			Oven drying Method (cm^3cm^{-3})
	Topp	LTPP	Pizarro	
1	0,2501	0,2394	0,2353	0,2375
2	0,1849	0,1864	0,1685	0,1694
4	0,1088	0,1242	0,0850	0,0839

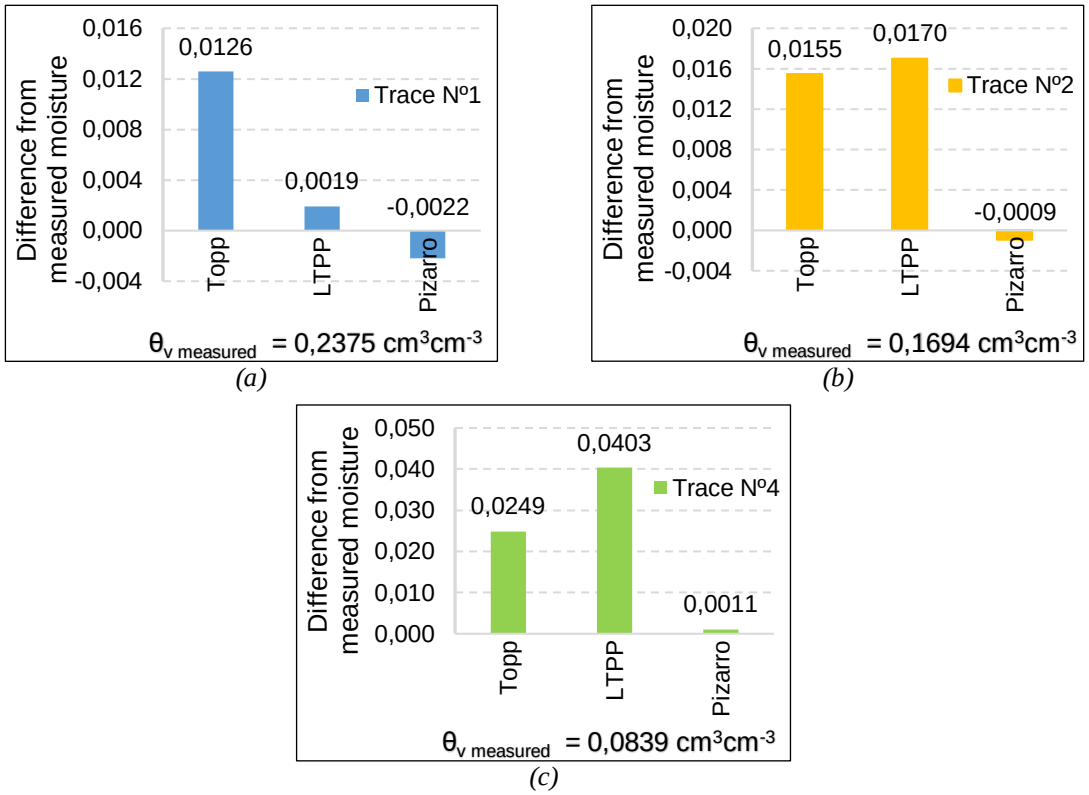

***Figure 8**. Differences between model-estimated and standard method-measured moistures.*

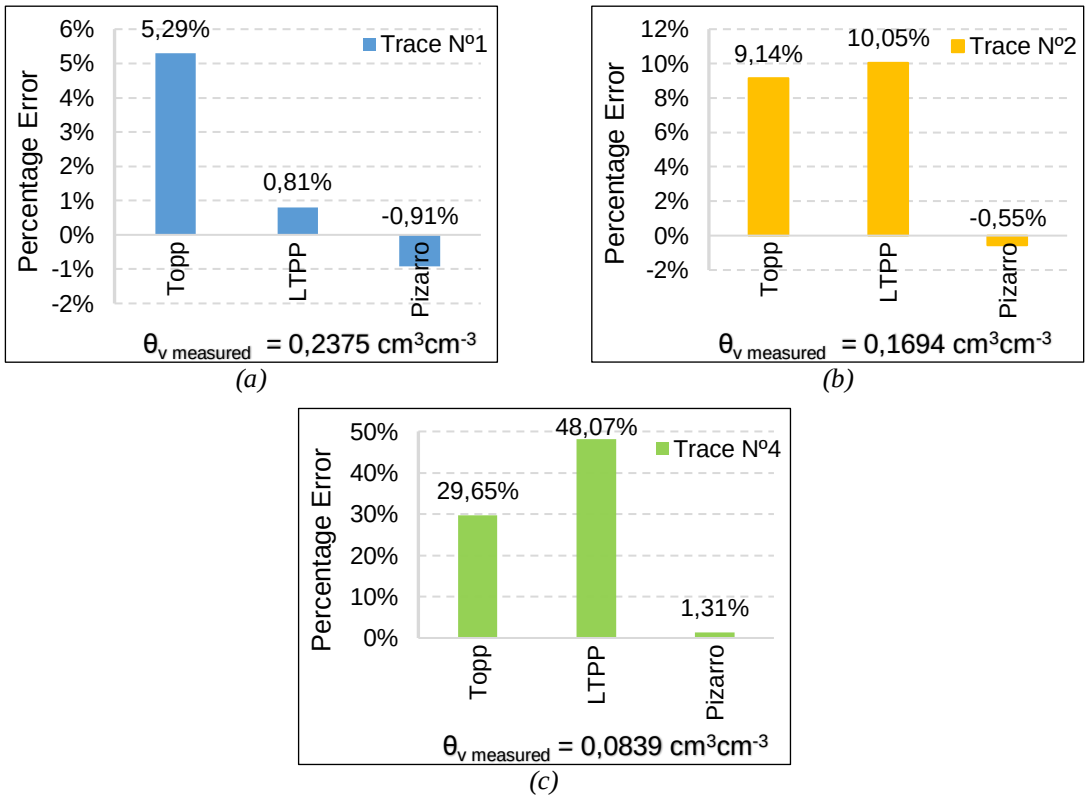

***Figure 9.** Percentage error that resulted from comparing the model-estimated and standard method-measured moistures.*

It is noteworthy from the graphs in Figure 8 and Figure ***9*** *that, compared to the measured moisture content of* $\theta_{v\,Measured} = 0{,}2375\ cm^3\ cm^{-3}$ *(Figure 8a) and (Figure Figure* ***9****a, the estimates using any of the three models can be considered satisfactory, with absolute percentage errors lower than 5,29%. In volumetric and gravimetric terms, the absolute differences between the moistures were less than 0,0126* $cm^3\ cm^{-3}$ *and 0,66%, respectively. Compared to the measured moisture content of* $\theta_{v\,Measured} = 0{,}1694\ cm^3\ cm^{-3}$ *(Figure 8.(b) and Figure* ***9****.(b)), the estimation using Pizarro's model showed the best result, with an absolute percentage error of less than 1%. However, the estimates using the other models were greater than 9%, which preliminarily suggests an overestimation in moisture prediction. For the measured moisture content of 0,0839* $cm^3\ cm^{-3}$ *(Figure 8c) and (Figure Figure* ***9*** *c), the percentage errors were close to 30% for the estimated moisture content with the Topp model, and close to 50% with the LTPP model. While Pizarro's model showed a moisture content with an absolute difference of 0,0011* $cm^3\ cm^{-3}$ *(*$\Delta w = 0{,}058\%$*), the other models showed differences above 0,0249* $cm^3\ cm^{-3}$ *(*$\Delta w \geq 1{,}30\%$*), showing overestimation in moisture prediction.*

It should be noted that the increased differences in predicting soil moisture as soil loses moisture between estimates using Pizarro's model versus Topp's model is due primarily to the influence of the specific mass of the soils that were used to generate the model. The dry density used to define Pizarro's model was 1,63 to 2,06 g cm^{-3}*, in contrast to the range of 1,32 to 1,44 g* cm^{-3} *used for Topp's model. The differences in moisture estimation when using the LTPP model are believed to be related to limitations in the accuracy of the same model. The high density of soils leads to a lower void ratio (e), which provides a greater contribution of the solid phase permittivity of the particles (*$\varepsilon_s = 3 - 5$*) in determining the total soil dielectric permittivity and a decrease in the contribution of the air phase (*$\varepsilon_a = 1$*) for low moisture contents and a reduction in the influence of the liquid phase (*$\varepsilon_w = 81$*) for high moisture contents, the effect of high density being more clear in the section of the curves fitted at lower moisture contents (*

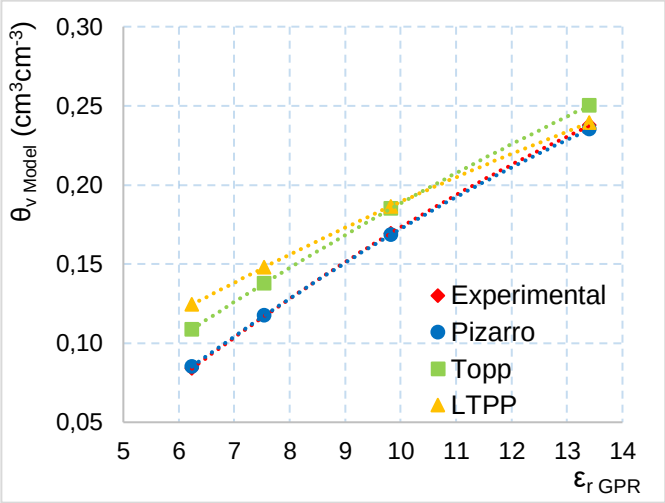

Figure 10*). It is a consensus among researchers that dielectric permittivity can be influenced by the dry density of the soil. The increase in density results in an increase in dielectric permittivity, mainly for low moisture contents (Jacobsen and Schjønning, 1993); (Gong, Cao and Sun, 2003); (Namdar-Khojasteh et al., 2012).*

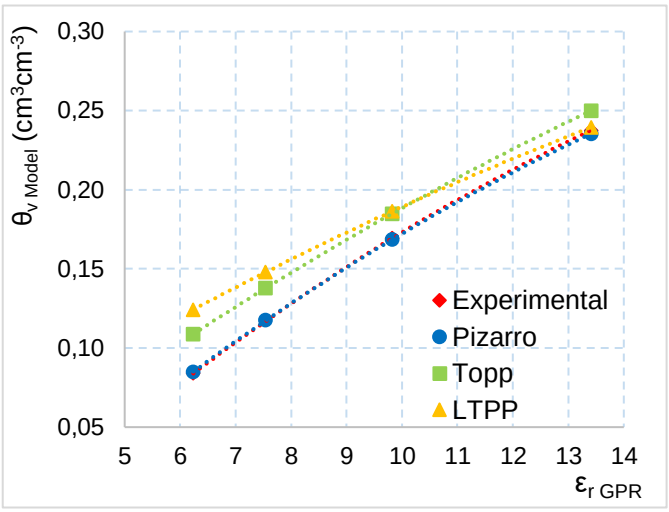

Figure 10*. Comparison of the experimental data obtained, and the curves fitted using Pizarro, Topp, and LTPP calibration models.*

From (

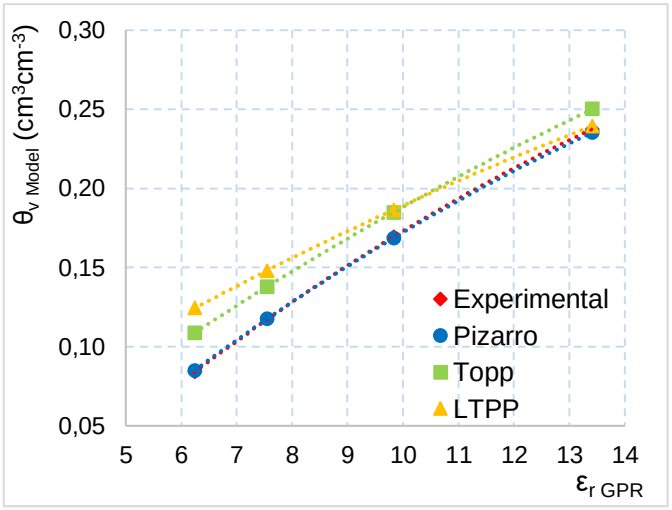

Figure 10*), it is worth noting the good performance of Pizarro's model, with excellent agreement between measured (oven drying method), estimated moisture contents, and the increase in moisture overestimation as dielectric permittivity decreases when the Topp and LTPP models were used.*

5. Conclusions

According to the results obtained and analyzed, the main conclusions of this research can be summarized in the following points:

- *The differences that resulted from the comparison between the moisture content estimated with GPR data and that measured by the oven drying method suggests that the GPR technique is a promising alternative, with satisfactory accuracy in the evaluation of moisture and that, with the standardized treatment of the data (GPR traces), it is possible to obtain the information (time or apparent length of the trace) for moisture variation control.*
- *In practical terms, GPR has shown sensitivity for monitoring changes in moisture content under controlled laboratory conditions. However, it is warned that with layers with thicknesses of only a few centimeters, small variations of tenths of nanoseconds in the definition of the travel time of the wave can lead*

to significant errors in the calculation of permittivity, affecting the estimate of moisture content in the same measurement.

- *It was found how the accuracy in predicting the moisture content using GPR data depends on the calibration model, highlighting the need for calibrated models for specific applications in civil engineering, which consider the geotechnical characteristics of tropical soil when compacted.*
- *It was verified the usefulness that the apparent length of the trace can have in the monitoring and analysis of moisture variation in compacted soil layers. The apparent length is another characteristic of the trace, which when normalized by a single value of arbitrary propagation velocity ($v_{p-arbitrary}$) in the study of different moisture conditions, facilitates the comparison and analysis of different traces, showing the decrease in apparent length as the moisture content also decreases.*

6. Acknowledgments

The authors are grateful to the following institutes and laboratories: Soil Mechanics Laboratory of the Department of Infrastructure and Environment (InfrA), Non-Destructive Research Laboratory (LIND) and Analytical Geochemistry Laboratory of the Institute of Geosciences, University of Campinas.

7. References

ABNT NBR 6458. (2016a). *Grãos de pedregulho retidos na peneira de abertura 4,8 mm - Determinação da massa específica, da massa específica aparente e da adsorção de água. Rio de Janeiro, Brazil (in Portuguese).*

ABNT NBR 6459. (2016b). *Solo - Determinação do limite de liquidez. Rio de Janeiro, Brazil (in Portuguese).*

ABNT NBR 7180. (2016c). *Solo - Determinação do limite de plasticidade. Rio de Janeiro, Brazil (in Portuguese).*

ABNT NBR 7181. (2016d). *Solo - Análise granulométrica. Rio de Janeiro, Brazil (in Portuguese).*

ABNT NBR 7182 (2016e) Solo - Ensaio de compactação. Rio de Janeiro, Brazil (in Portuguese).

Al-Qadi I.; Lahouar S.; Loulizi A.; Elseifi M.; Wilkes J. (2004). *Effective approach to improve pavement drainage layers. J. Transp. Eng. 130(5):658–664, doi: 10.1061/(ASCE)0733-947X(2004)130:5(658).*

Azevedo AM. (2007). *Considerações sobre a drenagem subsuperficial na vida útil dos pavimentos rodoviários. MSc Thesis, Department of Transport Engineering, Engineering School of the University of São Paulo, São Paulo, Brazil (in Portuguese).*

Bastos, J. (2013). *Influência da variação da umidade no comportamento de pavimentos da região metropolitana de Fortaleza. MSc Thesis, Department of Transport Engineering, Federal University of Ceará, Fortaleza, Brazil (in Portuguese).*

Benedetto A.; Tosti F, Bianchini CL.; D'Amico F. (2017). *An overview of ground-penetrating radar signal processing techniques for road inspections. Signal Process 132:201–209, doi: 10.1016/j.sigpro.2016.05.016.*

Benedetto A.; Benedetto F. (2002). *GPR experimental evaluation of subgrade soil characteristics for rehabilitation of roads. Proceedings of SPIE-The International Society for Optical Engineering 4758:708–714, doi:10.1117/12.462221.*

Benedetto A.; De Blasiis MR. (2010). *Applications of Ground Penetrating Radar to road pavement: State of the art and novelties. In: Paving Materials and Pavement Analysis. 2010, Shanghai: ASCE, 2010. 412-419, doi: 10.1061/41104(377)52.*

Berthelot C.; Podborochynski D.; Saarenketo T.; Marjerison B.; Prang C. (2010). *Ground-Penetrating Radar Evaluation of Moisture and Frost across Typical Saskatchewan Road Soils. Advances in Civil Engineering 1–9, doi: 10.1155/2010/416190.*

Curioni G. (2013). *Investigating the seasonal variability of electromagnetic soil properties using field monitoring data from Time-Domain Reflectometry probes. PhD Thesis, School of Civil Engineering, College of Engineering and Physical Sciences, University of Birmingham, Birmingham, UK.*

D'Amico F.; Guattari C.; Benedetto A. (2010). *GPR signal processing in frequency domain using Artificial Neural Network for water content prediction in unsaturated subgrade. In: International Conference on Ground Penetrating Radar, 13th, 2010, Lecce, Italy*.

Daniels JJ. (2010). *Ground Penetrating Radar Fundamentals. 1st ed. Ohio: Department of Geological Sciences, The Ohio State University, Prepared as an appendix to a Report to the US EPA, Region V*.

DNER-ME 256/94. (1994a). *Solos compactados com equipamento miniatura - Determinação da perda de massa por imersão. Rio de Janeiro, Brazil (in Portuguese).*

DNER-ME 258/94. (1994b). *Solos compactados em equipamento miniatura - Mini-MCV. Rio de Janeiro, Brazil (in Portuguese).*

DNER-CLA 259/96. (1996). *Classificação de solos tropicais para finalidades rodoviárias utilizando corpos de prova compactados em equipamento miniatura. Rio de Janeiro, Brazil (in Portuguese).*

Ekblad J.; Isacsson U. (2007). *Time-domain reflectometry measurements and soil-water characteristic curves of coarse granular materials used in road pavements. Canadian Geotechnical Journal 44(7):858–872, doi: 10.1139/t07-024.*

Evans R.; Frost M.; Morrow R. (2012). *Assessing the influence of moisture on the dielectric properties of asphalt. In: International Conference on Ground Penetrating Radar, 14th, 2012, Shanghai, China: IEEE, 2012. p. 536-541. Available in: <https://www.scopus.com/inward/record.uri?eid=2-s2.0-84866790418&partnerID=40&md5=8224bc1f8b97196375f1533342db73d3>.*

Friedman SP. (2011). *Electrical Properties of Soils. In Encyclopedia of Agrophysics, Gliński, J., Horabik, J., Lipiec, J., Orgs. Dordrecht: Springer, Netherlands, 2011, p. 242–255, doi: 10.1007/978-90-481-3585-1_48.*

Gong Y.; Cao Q.; Sun Z. (2003). *The effects of soil bulk density, clay content and temperature on soil water content measurement using time-domain reflectometry. Hydrological Processes 17(18):3601–3614, doi: 10.1002/hyp.1358.*

Grote K.; Hubbard S.; Harvey J, Rubin Y. (2005). *Evaluation of infiltration in layered pavements using surface GPR reflection techniques. Journal of Applied Geophysics 57(2):129–153, doi: 10.1016/j.jappgeo.2004.10.002.*

Grote K.; Hubbard S.; Rubin Y. (2002). *GPR monitoring of volumetric water content in soils applied to highway construction and maintenance. The Leading Edge 21(5):482–504, doi: 10.1190/1.1481259.*

Huisman JA.; Hubbard SS.; Redman JD.; Annan AP. (2003). *Measuring Soil Water Content with Ground Penetrating Radar. Vadose Zone Journal 2(4):476–491, doi: 10.2136/vzj2003.4760.*

Jacobsen OH.; Schjønning P. (1993). *A laboratory calibration of time domain reflectometry for soil water measurement including effects of bulk density and texture. Journal of Hydrology 151(2–4):147–157, doi: 10.1016/0022-1694(93)90233-Y.*

Jiang Y.; Tayabji S. (1999). *Evaluation of in situ moisture content at long-term pavement performance seasonal monitoring program sites. Transportation Research Record: Journal of the Transportation Research Board 1655(99–0395):118–126, doi: 10.3141/1655-16.*

Larrahondo JM.; Atalay F.; McGillivray AV.; Mayne PW. (2008). *Evaluation of road subsurface drain performance by geophysical methods. In: Geocongress 2008: Geosustainability and Geohazard Mitigation, New Orleans, Lousiana: ASCE, 2008. p. 538-545, Available in: <https://www.scopus.com/inward/record.uri?eid=2-s2.0-*

66549102115&doi=10.1061%2f40971%28310%2967&partnerID=40&md5=245959d0579b0d8d65d33c7d15ee3cd0>.

Loulizi A. (2001). *Development of Ground Penetrating Radar Signal Modeling and Implementation for Transportation Infrastructure Assessment. PhD Thesis, Faculty of the Virginia Polytechnic, Institute and State University, Blacksburg, Virginia, USA.*

Mohamed A. (2008). *Impact of soil magnetic permeability on water content prediction using TDR. In: The 12th International Conference of International Association for Computer Methods and Advances in Geomechanics (IACMAG). Goa, India: Citeseer, 2008. p. 1365-1372.*

Muller W. (2016). *Characterising moisture within unbound granular pavements using multi-offset Ground Penetrating Radar. PhD Thesis, School of Civil Engineering, University of Queensland, Queensland, Australia*.

Nadler A.; Dasberg S.; Lapid I. (1991). *Time domain reflectometry measurements of water content and electrical conductivity of layered soil columns. Soil Science Society of America Journal 55(4):938–943, doi: 10.2136/sssaj1991.03615995005500040007x.*

Namdar-Khojasteh D.; Shorafa M.; Omid M. (2012). *Evaluation of dielectric constant by clay mineral and soil physico-chemical properties. African journal of Agricultural research 7(2):170–176, doi: 10.5897/AJAR10.346.*

Pereira AC. (2003). *Influência da drenagem subsuperficial no desempenho de pavimentos asfálticos. MSc Thesis, Department of Transport Engineering, Engineering School of the University of São Paulo, São Paulo, Brazil (in Portuguese).*

Pizarro I.; Françoso M.; De Almeida L.; Matsura E. (2020). *Calibration of an empirical model for moisture content assessment and monitoring in compacted tropical soils used in the subgrade of road pavements. Revista Ingeniería de Construcción 35(3):275–286, doi: 10.4067/S0718-50732020000300275.*

Plati C.; Loizos A. (2013). *Estimation of in-situ density and moisture content in HMA pavements based on GPR trace reflection amplitude using different frequencies. Journal of Applied Geophysics 97:3–10, doi: 10.1016/j.jappgeo.2013.04.007.*

Roth C.; Malicki M.; Plagge R. (1992). *Empirical evaluation of the relationship between soil dielectric constant and volumetric water content as the basis for calibrating soil moisture measurements by TDR. European Journal of Soil Science 43(1):1–13, doi: 10.1111/j.1365-2389.1992.tb00115.x.*

Saarenketo T. (2006). *Electrical properties of road materials and subgrade soils and the use of Ground Penetrating Radar in traffic infrastructure surveys. PhD Thesis, Faculty of Science, University of Oulu, Oulun Yliopisto, Oulu.*

Suzuki CY.; Azevedo AM.; Júnior FI. (2013). *Drenagem subsuperficial de pavimentos: conceitos e dimensionamento, 1st ed.; Oficina de Textos; São Paulo, Brazil (in Portuguese).*

Topp GC.; Davis J.; Annan AP. (1980). *Electromagnetic determination of soil water content: Measurements in coaxial transmission lines. Water resources research 16(3):574–582, doi: 10.1029/WR016i003p00574.*

Van Dam RL.; Schlager W.; Dekkers MJ.; Huisman JA. (2002). *Iron oxides as a cause of GPR reflections. Geophysics 67(2):536–545, doi: 10.1190/1.1468614.*

Wai-Lok Lai W.; Dérobert X.; Annan P. (2017). *A review of Ground Penetrating Radar application in civil engineering: A 30-year journey from Locating and Testing to Imaging and Diagnosis. NDT & E International 1–22, doi: 10.1016/j.ndteint.2017.04.002.*